

hep-ph/0205286
 RM3-TH/02-07
 DFTT 13/02
 GeF/TH/4-02
 UB-ECM-FP-02-12

Determination of α_s from scaling violations of truncated moments of structure functions

Stefano Forte,^a José I. Latorre,^b Lorenzo Magnea^c and Andrea Piccione^d

^aINFN, Sezione di Roma Tre
 Via della Vasca Navale 84, I-00146 Rome, Italy

^bDepartament d'Estructura i Constituents de la Matèria,
 Universitat de Barcelona, Diagonal 647, E-08028 Barcelona, Spain

^cDipartimento di Fisica Teorica, Università di Torino and INFN, Sezione di Torino
 Via P. Giuria 1, I-10125 Torino, Italy

^dDipartimento di Fisica, Università di Genova and INFN, Sezione di Genova,
 Via Dodecaneso 33, I-16146 Genova, Italy

Abstract

We determine the strong coupling $\alpha_s(M_Z)$ from scaling violations of truncated moments of the nonsinglet deep inelastic structure function F_2 . Truncated moments are determined from BCDMS and NMC data using a neural network parametrization which retains the full experimental information on errors and correlations. Our method minimizes all sources of theoretical uncertainty and bias which characterize extractions of α_s from scaling violations. We obtain $\alpha_s(M_Z) = 0.124 \pm_{-0.007}^{+0.004}$ (exp.) $\pm_{-0.004}^{+0.003}$ (th.).

May 2002

1 Introduction

As the predictions of QCD become increasingly precise and more high quality data are available, the theoretical uncertainties associated with the analysis of the data are more and more often found to be dominant, and have thus come under increased scrutiny [1]. The determination of the QCD coupling $\alpha_s(M_Z)$ [2] from scaling violations of deep inelastic structure functions is perhaps the simplest and most fundamental example of this situation. In principle, deep inelastic scattering would be expected to provide a theoretically solid and experimentally clean way of determining $\alpha_s(M_Z)$. In practice, however, the situation is far from satisfactory [3], as revealed by the lack of stability of the value of α_s obtained through this procedure.

The main source of difficulties can be traced to the fact that conventional extractions of α_s from scaling violations of structure functions involve a simultaneous determination of parton distributions of the nucleon. The error on α_s , therefore, gets tangled with the uncertainty on parton distributions, which is notoriously difficult to assess, and subject to a variety of sources of theoretical bias [1]. This is a consequence of the fact that the evolution equations of perturbative QCD [4], which govern scaling violations, can only be solved analytically in compact form by taking Mellin moments, which diagonalize the evolution operator. In practice, however, Mellin moments are not directly measurable, since their determination would require the availability of data taken at arbitrarily large center-of-mass energy. The problem is circumvented by solving directly the momentum-space Altarelli-Parisi [5] equations, which, however, usually entails the construction of a parton parametrization.

Such an undertaking thus runs into two difficulties. First, a parton parametrization is routinely constructed by assuming a functional form for parton distributions, and fitting the corresponding free parameters. The choice of a functional form, however, introduces a theoretical bias, which is potentially large, and whose size is very difficult to assess [6]. For example, choices of functional form based on “QCD expectations” may well give a poor representation of unexpected or unconventional behaviors of the distributions. Furthermore, any given parametrization constrains the form of the distribution near and beyond the boundary of the region where data are available: whenever the data are not very precise, it can be seen [7] that the results obtained for observable quantities may depend significantly on the form of the parametrization.

Second, it is quite difficult to estimate precisely the error on parton distributions, and even harder to propagate this error to quantities which depend upon them. Indeed, a generic observable (such as a Mellin moment, or a cross section) is a functional of parton distributions, which in general depends on it in a complicated, nonlocal way. Thus, on the one hand it is difficult to extract the errors on parton distributions from errors on the data, on the other hand it is difficult to propagate errors on parton distributions to quantities calculated from them. At the very least, the full information on experimental errors and correlations should be used, but it may also turn out that conventional techniques of linear error propagation fail. These difficulties could only be overcome if one were able to obtain a reliable and unbiased representation of the probability measure in the functional space of parton distributions [8], as determined by the available experimental information.

In this paper, we approach the determination of α_s in a way which bypasses these difficulties, by combining two techniques which have recently been proposed and implemented in the context

of the analysis of DIS data: the use of evolution equations for truncated Mellin moments of parton distributions [9–11], and the determination of the probability measure in the space of deep inelastic structure functions by means of neural networks [12].

Truncated moments are defined as Mellin moments with the integration range restricted to the subset $x_0 < x < 1$ of the kinematically allowed range $0 < x < 1$. Unlike ordinary Mellin moments, they are measurable quantities, since the small x region is excluded. The evolution equations which they satisfy turn out to be a system of coupled ordinary linear differential equations, which can be truncated to finite accuracy to yield a closed system. The evolution equations for truncated moments have been derived, and explicitly solved at next-to-leading order in the nonsinglet [9] and singlet [10] sectors. The numerical accuracy of the approximate solutions has been studied and improved upon by means of suitable techniques [11], and is equal or better than that of standard numerical solutions of Altarelli-Parisi equations [1].

Given an experimental determination of truncated moments at more than one scale, one can then determine α_s directly by comparing computed and measured scaling violations. In the nonsinglet sector, there is only one independent structure function, say F_2 , and scaling violations are fully determined by α_s and an initial condition, given by the values of the truncated moments of F_2 at a reference scale: therefore one does not have to use a parton parametrization.

In practice, however, a sufficiently accurate determination of truncated moments of the nonsinglet F_2 and associated errors and correlations cannot be obtained by simply binning and summing data points: the coverage and precision of the data are not sufficient for this purpose. Rather, in order to fully exploit the available experimental information, it is necessary to construct a parametrization of the structure function in the kinematic region where data are available. This clearly leads back to the same difficulties encountered when constructing a parton parametrization. The problem, however, can now be overcome, since an unbiased determination of the probability density in the space of structure functions, based on available experimental data, has been constructed in Ref. [12].

The representation of the probability density given in Ref. [12] takes the form of a set of neural networks, trained on an ensemble of Monte Carlo replicas of the experimental data, which reproduce their probability distribution. The parametrization is unbiased, since neural networks do not require the choice of a specific functional form, and it interpolates between data points, imposing smoothness constraints in a controllable way. Information on experimental errors and correlations is incorporated in the Monte Carlo sample, so that errors on truncated moments and correlations between them can be determined without having to use linearized error propagation. The parametrization combines all the available experimental information, so that statistical errors are minimized, but it also correctly reproduces the loss of accuracy incurred when extrapolating outside the kinematical region where data are available.

Hence, we can obtain an unbiased evaluation of truncated moments, and then use this to determine α_s directly without any further assumptions. We end up with a determination of α_s where all sources of uncertainty related to the method of analysis are under control, and the only theoretical uncertainty is related to the lack of knowledge of the anomalous dimensions beyond next-to-leading order. This gives us a bias-free determination of α_s , and simultaneously illustrates the power of a method of analysis based on the direct knowledge of a probability density in a space of functions.

This paper is organized as follows: in section 2 we will review the method of truncated

moments [9–11], emphasizing the issues of numerical accuracy which are relevant to the rest of the paper; in section 3 we will introduce the neural network parametrization of DIS structure functions developed in Ref. [12]; section 4 contains the details of our fitting procedure and our result for the strong coupling $\alpha_s(M_Z)$: we explain our data selection, our choice of fitting architecture, our error estimate and the consistency tests that we performed; finally, section 5 summarizes our conclusions and discusses possible extensions of our work.

2 Truncated moments of parton distributions

We determine the strong coupling from the scale dependence of the nonsinglet deep inelastic structure function

$$F_2^{NS}(x, Q^2) = F_2^p(x, Q^2) - F_2^d(x, Q^2) . \quad (2.1)$$

In the DIS scheme [13], F_2^{NS} is expressed directly in terms of the nonsinglet combination of quark distribution, according to

$$F_2^{NS}(x, Q^2) = \sum_{i=1}^{n_f} e_i^2 \left[q_i(x, Q^2) + \bar{q}_i(x, Q^2) \right]_{p-n} . \quad (2.2)$$

The scale dependence of F_2 is thus given by the evolution equation for nonsinglet quark distributions, henceforth denoted simply by $q(x, \mu^2)$,

$$\mu^2 \frac{d}{d\mu^2} q(x, \mu^2) = \frac{\alpha_s(\mu^2)}{2\pi} \int_x^1 \frac{dy}{y} P\left(\frac{x}{y}, \alpha_s(\mu^2)\right) q(y, \mu^2) , \quad (2.3)$$

where $P(z, \alpha_s)$ is the appropriate evolution kernel.

2.1 Evolution equations for truncated moments

Consider now the truncated Mellin moment of the quark distribution

$$q_n(x_0, \mu^2) \equiv \int_{x_0}^1 dx \, x^{n-1} q(x, \mu^2) . \quad (2.4)$$

The evolution equation for truncated moments is easily found to be

$$\mu^2 \frac{d}{d\mu^2} q_n(x_0, \mu^2) = \frac{\alpha_s(\mu^2)}{2\pi} \int_{x_0}^1 dy \, y^{n-1} q(y, \mu^2) G_n\left(\frac{x_0}{y}; \alpha_s(\mu^2)\right) , \quad (2.5)$$

where G_n is the truncated moment of the splitting function

$$G_n(x, \alpha_s) = \int_x^1 dz \, z^{n-1} P(z, \alpha_s) . \quad (2.6)$$

Note that the function $G_n(x, \alpha_s)$ is analytic on the real axis in the interval $0 \leq x < 1$, while it has integrable singularities at $x = 1$ as a consequence of the presence of $+$ distributions in the kernel $P(z, \alpha_s)$ at all perturbative orders.

We can turn eq. (2.5) into a set of coupled linear differential equations by expanding $G(x_0/y, \alpha_s)$ in powers of y around $y = 1$ as

$$G_n\left(\frac{x_0}{y}, \alpha_s\right) = \sum_{p=0}^{\infty} \frac{1}{p!} g_p^{(n)}(x_0, \alpha_s) (y-1)^p. \quad (2.7)$$

Because the singularities of $G_n(x_0/y, \alpha_s)$ at $y \rightarrow x_0$ are integrable, one can substitute eq. (2.7) into eq. (2.5) and integrate term by term, obtaining a convergent series. It is then legitimate to truncate the sum in eq. (2.7) at a finite order $p = M$, with the result

$$G_n\left(\frac{x_0}{y}, \alpha_s\right) = \sum_{p=0}^M c_{p,n}^{(M)}(x_0, \alpha_s) y^p + O\left[(y-1)^{M+1}\right], \quad (2.8)$$

where

$$c_{p,n}^{(M)}(x_0, \alpha_s) = \sum_{k=p}^M \frac{(-1)^{p+k} g_k^{(n)}(x_0, \alpha_s)}{p!(k-p)!}. \quad (2.9)$$

The evolution equation for truncated moments then becomes [9]

$$\mu^2 \frac{d}{d\mu^2} q_n(x_0, \mu^2) = \frac{\alpha_s(\mu^2)}{2\pi} \sum_{p=0}^M c_{p,n}^{(M)}(x_0, \alpha_s) q_{n+p}(x_0, \mu^2), \quad (2.10)$$

and is thus given by a set of coupled linear differential equations. The anomalous dimension matrix $c_{p,n}^{(M)}(x_0, \alpha_s)$ couples each truncated moment q_n to all truncated moments q_k with $k \geq n$. The evolution equation for the k -th moment can be made arbitrarily accurate by taking M to be sufficiently large.

2.2 Solution of the evolution equations

The coupled evolution of the moments q_k , with $n \leq k \leq n+M$, can be solved to determine the value of q_n at different scales, if the system in eq. (2.10) closes, *i.e.* if it is legitimate to include a decreasing number of terms in the evolution equation of increasingly higher moments. In Ref. [9] it was shown that this is indeed the case, because the matrix elements of $c_{p,n}^{(M)}(x_0, \alpha_s)$ decrease rapidly as one moves away from the diagonal, so that the accuracy of the truncated evolution kernel actually improves with increasing order of the moment, even if one less term is included when the order is increased by one unit.

Having chosen the values for n and M , we can introduce the simplified notation

$$\begin{aligned} C_{kl}(\alpha_s) &= c_{l-k,k}^{(M-k+n)}(x_0, \alpha_s) \quad (n+M \geq l \geq k \geq n), \\ C_{kl}(\alpha_s) &= 0 \quad (n \leq l < k \leq n+M), \end{aligned} \quad (2.11)$$

in terms of which the system of equations to be solved reads simply

$$\mu^2 \frac{d}{d\mu^2} q_k(x_0, \mu^2) = \frac{\alpha_s(\mu^2)}{2\pi} \sum_{l=n}^{n+M} C_{kl}(\alpha_s) q_l(x_0, \mu^2), \quad (2.12)$$

with $n \leq k \leq n + M$. Expanding $C_{kl}(\alpha_s)$ in powers of α_s to next-to-leading order, one can now solve eq. (2.12) by standard perturbative methods. The task is considerably simplified by the fact that the matrix of coefficients, $C_{kl}(\alpha_s)$, is upper triangular, so that the eigenvalues are exactly the diagonal elements C_{kk} , and the eigenvectors are easily computed by means of a recursion relation. The explicit solution is given in Ref. [9].

In practice, the numerical implementation of the solution may be problematic if a high accuracy is required for low moments. Indeed, it turns out that when $x_0 = 0.1$ the value of M which is needed to achieve an accuracy at the few percent level on the evolution of the n -th truncated moment is typically of order $M \gtrsim 100$ for the lowest moments, $n = 1, 2$ (when $n < 1$ the convolution integral in eq. (2.5) diverges), even though it rapidly decreases for higher moments. Such a large value of M leads to numerical difficulties, due to the fact that the matrix elements $C_{kl}(\alpha_s)$ become very small when $l \gg k$.

2.3 Improved solution

An improved solution to the evolution equation, which overcomes the problems related to the slow convergence of the expansion of the evolution kernel for low moments, can however be derived [11]. The origin of the problem is easily tracked to the logarithmic singularities left over in the function $G_n(x_0/y, \alpha_s)$, for $y \rightarrow x_0$, as a consequence of the presence of $+$ distributions in the evolution kernel $P(z, \alpha_s)$, for $z \rightarrow 1$. For the lowest moments, the integration over y is dominated by small values of y , $y \sim x_0$, where the function G_n is in turn dominated by the logarithmic singularity, and not well approximated by a low-order truncation of its Taylor expansion around $y = 1$.

To solve the problem, one can integrate by parts the right hand side of eq. (2.5), obtaining

$$\begin{aligned} \int_{x_0}^1 dy y^{n-1} q(y, \mu^2) G_n\left(\frac{x_0}{y}, \alpha_s\right) &= \left[\tilde{G}_n(x_0, y; \alpha_s) y^{n-1} q(y, Q^2) \right]_{x_0}^1 \\ &- \int_{x_0}^1 dy \tilde{G}_n(x_0, y; \alpha_s) \frac{d}{dy} \left(y^{n-1} q(y, Q^2) \right) , \end{aligned} \quad (2.13)$$

where

$$\tilde{G}_n(x_0, y; \alpha_s) = \int_{x_0}^y dz G_n\left(\frac{x_0}{z}, \alpha_s\right) . \quad (2.14)$$

In the definition of \tilde{G}_n the freedom to fix the lower limit of integration, which is independent of y , has been exploited, so that the function \tilde{G}_n satisfies $\tilde{G}_n(x_0, x_0; \alpha_s) = 0$, as well as

$$\tilde{G}_n(x_0, y; \alpha_s) = y G_n\left(\frac{x_0}{y}, \alpha_s\right) - x_0 G_{n-1}\left(\frac{x_0}{y}, \alpha_s\right) ; \quad (2.15)$$

furthermore, the coefficients of the Taylor expansion of \tilde{G}_n around $y = 1$, defined as in eq. (2.7), satisfy, in obvious notations,

$$\tilde{g}_p^{(n)}(x_0, \alpha_s) = g_{p-1}^{(n)}(x_0, \alpha_s) . \quad (2.16)$$

The integration region $y \sim x_0$ is now suppressed, and a faster rate of convergence when \tilde{G}_n is expanded around $y = 1$ is expected. Repeating the procedure that leads to eq. (2.12) one

gets [11]

$$\begin{aligned} \mu^2 \frac{d}{d\mu^2} q_n(x_0, \mu^2) &= \frac{\alpha_s(\mu^2)}{2\pi} \left[x_0^{n-1} q(x_0, \mu^2) \sum_{p=0}^M \frac{1}{p!} \tilde{g}_p^{(n)}(x_0, \alpha_s) (x_0 - 1)^p \right. \\ &\quad \left. + \sum_{l=1}^M C_{nl}(\alpha_s) q_l(x_0, \mu^2) \right] . \end{aligned} \quad (2.17)$$

The coefficients $C_{nl}(\alpha_s)$ are given in eq. (2.11). The first term on the right hand side of eq. (2.17) is responsible for the faster convergence of the expansion to the exact result: it vanishes as $M \rightarrow \infty$, as it must, since it reconstructs $\tilde{G}_n(x_0, x_0; \alpha_s) = 0$.

Eq. (2.17), however, cannot be used directly: as the right-hand side of the equation depends on the value of $q(x_0, \mu^2)$, we do not get a closed system of equations. This obstacle can be circumvented by noting [11] that $q(x_0, \mu^2)$ itself can be expanded over a basis of truncated moments, and, specifically, a finite set of them is sufficient to give an accurate determination of $q(x_0, \mu^2)$. To see this, expand the quark distribution in Taylor series about a selected point, say $y_0 = (1 + x_0)/2$ (note that $y_0 > (1 + x_0)/2$ is not allowed since $y = 1$ is an essential singularity of all parton distributions)

$$q(x, \mu^2) = \sum_{k=1}^{\infty} \eta_k(\mu^2) (x - y_0)^{k-1} . \quad (2.18)$$

Truncated moments are then given by

$$q_j(x_0, \mu^2) = \sum_{k=1}^{\infty} \beta_{jk} \eta_k(\mu^2) , \quad (2.19)$$

where

$$\beta_{jk} = \int_{x_0}^1 dx x^{j-1} (x - y_0)^{k-1} . \quad (2.20)$$

The infinite matrix β_{jk} can be approximated by truncating it to a square $N \times N$ matrix $\tilde{\beta}_{jk}$, which is easily computed and inverted. One finds then an approximate expression for $q(x_0, \mu^2)$, given by

$$q(x_0, \mu^2) = \sum_{k=1}^N \sum_{j=1}^N \tilde{\beta}_{kj}^{-1} q_j(x_0, \mu^2) (x_0 - y_0)^{k-1} . \quad (2.21)$$

The error introduced by the truncation of the matrix β_{jk} has been studied, as a function of N , in Ref. [11]. It turns out that a satisfactory accuracy (at the 0.1% level) can be reached already for $N \sim 5$, while in practice the inversion of the matrix $\tilde{\beta}_{jk}$ becomes numerically difficult only for $N > 10$ (as easily verified, the matrix is ill-conditioned). The method is thus viable and does not lead to loss of accuracy.

Combining eq. (2.17) and eq. (2.21), we get the final form for the evolution equation, which replaces eq. (2.12), namely

$$\mu^2 \frac{d}{d\mu^2} q_k(x_0, \mu^2) = \frac{\alpha_s(\mu^2)}{2\pi} \sum_{l=n}^{n+M} \left[C_{kl}(\alpha_s) + D_{kl}^{(N)}(\alpha_s) \right] q_l(x_0, \mu^2) , \quad (2.22)$$

where

$$D_{kl}^{(N)}(\alpha_s) = x_0^{k-1} \left[\sum_{p=0}^M \frac{1}{p!} \tilde{g}_p^{(k)}(x_0, \alpha_s) (x_0 - 1)^p \right] \left[\sum_{r=1}^N \tilde{\beta}_{rl}^{-1} (x_0 - y_0)^{r-1} \right]. \quad (2.23)$$

Once again, eq. (2.22) can be solved by expanding $C_{kl}(\alpha_s)$ and $D_{kl}^{(N)}(\alpha_s)$ to next-to-leading order in α_s , and then using well-known perturbative methods. A compact expression for the solution is given in Refs. [10, 11]. The price to pay for the faster convergence of eq. (2.22) is that the evolution matrices are no longer triangular. This implies that all truncated moments with $n \geq 1$ must be used as initial conditions in order to compute the evolution of any moment. As a consequence, diagonalization has to be performed numerically rather than analytically. In practice, however, this does not lead to any numerical difficulties: as shown in Ref. [11], an accuracy at the few percent level on the evolution can be achieved for any truncated moment with $M \sim 10$, a size at which numerical diagonalization is not difficult. It is important to notice that all the approximations that have been introduced in order to make the problem amenable to a numerical solution are under theoretical control, and the accuracy achieved can be precisely estimated and can be improved upon if the need arises.

3 Neural network parametrization of deep inelastic structure functions

Ideally, a parametrization of structure functions must incorporate all the information contained in the experimental measurements, *i.e.* their central values, their statistical and systematic errors, and their correlations; furthermore, it must interpolate between them without introducing any bias. Several approaches to this problem have been proposed, in the context of fitting parton distributions: χ^2 -minimization of a fixed functional form coupled to error propagation through the covariance matrix, and various improvements thereof [14]; projection over bases of orthogonal polynomials [15]; or Monte Carlo sampling coupled to Bayesian inference [8]. Here we will follow the method of Ref. [12], where an unbiased extraction of the probability measure in the space of structure functions is performed, based on a coordinated use of Monte Carlo generation of data and neural network fits.

3.1 Experimental data

Since we are interested in the nonsinglet structure function F_2 , we need a simultaneous measurement of this structure function for proton and deuterium targets. We will use the data of the New Muon Collaboration (NMC) [16] and of the BCDMS (Bologna-CERN-Dubna-Munich-Saclay) Collaboration [17], which provide a simultaneous determination of the proton and deuteron structure functions in the same kinematic region, and provide the full set of correlated experimental systematics for these measurements. Earlier data from SLAC are not competitive with these in terms of accuracy and kinematic coverage. The more recent HERA data are available in a much wider kinematic region, but only for proton targets. Another set of joint proton and deuteron measurements was performed by the E665 Collaboration [18]. These data however are mostly concentrated at low Q^2 (and low x), and thus are not relevant for

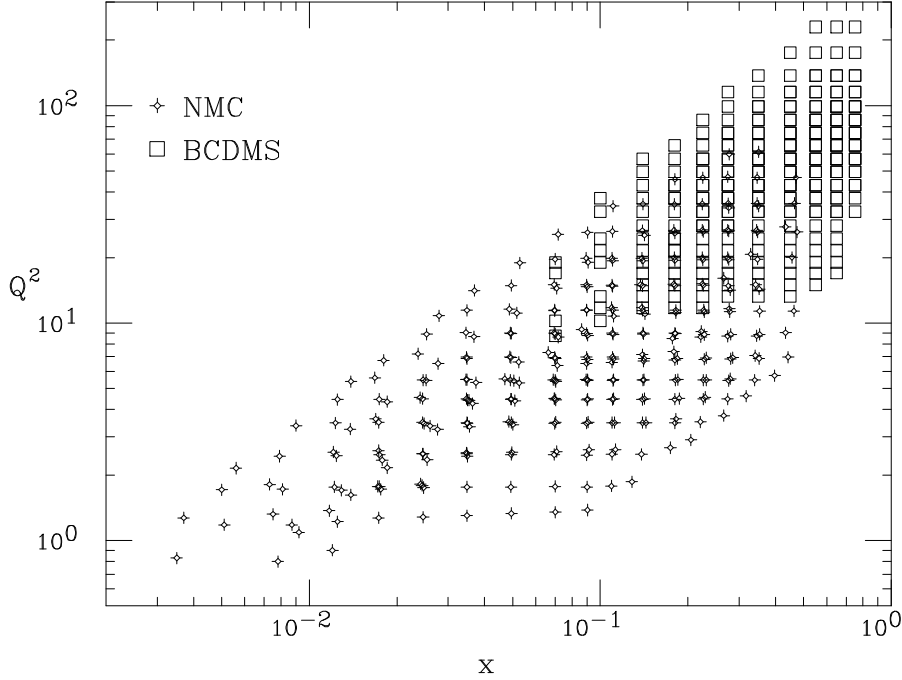


Figure 1: NMC and BCDMS kinematic range.

perturbative QCD applications. The kinematic coverage of the data which we include in our analysis is displayed in Fig. 1. Altogether our parametrization is based on $N_{dat} = 552$ experimental points for the nonsinglet structure function, obtained as difference of pairs of proton and deuteron data according to eq. (2.1). Henceforth, $F_i^{(exp)}$ will denote the i -th data point $F_2^{NS}(x_i, Q^2)$.

3.2 Probability measure in the space of structure functions

The experimental data give us a probability measure in an N_{dat} -dimensional space, assumed to be multigaussian. In order to extract from it a parametrization of the desired structure function we must turn this measure into a measure $\mathcal{P}[F_2]$ in a space of functions. Once such a measure is constructed, the expectation value of any observable $\mathcal{F}[F_2(x, Q^2)]$ can be found by computing the weighted average

$$\langle \mathcal{F}[F_2(x, Q^2)] \rangle = \int \mathcal{D}F_2 \mathcal{F}[F_2(x, Q^2)] \mathcal{P}[F_2] . \quad (3.24)$$

Errors and their correlations can also be obtained from this measure, by considering higher moments of the same observable with respect to the probability distribution.

The determination of an infinite-dimensional measure from a finite set of data points is an ill-posed problem, unless one introduces further assumptions. For instance, one may assume a fixed functional form [14], in which case the problem is reduced to the determination of a

finite set of parameters, or one may project over a basis of orthogonal polynomials [15], and choose a particular truncation of the *a priori* infinite set of basis functions. In the approach of Ref. [12], neural networks are used as interpolating functions, so that the only assumption is the smoothness of the structure function. Neural networks can fit any continuous function through a suitable training; smoother functions require a shorter training and less complex networks. Hence, an ideal degree of smoothness can be established on the basis of a purely statistical criterion (such as having reached a satisfactory goodness-of-fit) without need for further assumptions.

3.3 Fitting strategy

The construction of the probability measure is done in two steps: first, a set of Monte Carlo replicas of the original data set is generated. This gives a representation of the probability density $\mathcal{P}[F_2]$ at points (x_i, Q_i^2) where data are available. Then, a neural network is fitted to each replica. The ensemble of neural networks gives a representation of the probability density for all (x, Q^2) : when interpolating between data the uncertainty will be kept under control by the smoothness constraint, but it will become increasingly more sizable when extrapolating away from the data region.

The $k = 1, \dots, N_{rep}$ replicas of the data are generated as

$$F_i^{(art)(k)} = (1 + r_{i,N}^{(k)} \sigma_{i,N}) \left[F_i^{(exp)} + \frac{\sum_a r_{i,a}^{(k)} f_{i,a}}{100} F_i^{(exp)} + r_{i,s} \sigma_{i,s}^{(k)} \right], \quad (3.25)$$

where $F_i^{(exp)} \equiv F_2(x_i, Q_i^2)$ are the original data, $f_{i,a}$ are the experimental systematic errors, given in percentage, $\sigma_{i,N}$ is the experimental normalization error, $\sigma_{i,s}$ is the experimental statistical error, while $r_{i,a}^{(k)}$, $r_{i,s}^{(k)}$ and $r_{i,N}^{(k)}$ are univariate gaussian numbers. When two data points share a correlated error or normalization, the same gaussian number is used. In Ref. [12], a set of $N_{rep} = 1000$ replicas of this form has been generated, and it has been verified that central values, errors and correlations of the original experimental data are well reproduced by taking the relevant averages over a sample of this size. The kinematic bound $F_2(1, Q^2) = 0$ has been implemented by adding a number of artificial data points at $x = 1$ with carefully adjusted errors.

Each set of generated data is fitted by an individual neural network. A neural network [19] is a function of a number of parameters, which fix the strength of the coupling between neurons and the thresholds of activation for each neuron. The architecture of the network is chosen to be redundant for the given problem, *i.e.* the number of parameters is rather larger than the minimum needed to get a good fit. The parameters are then fitted by minimizing an error function. The fit is done using the technique of learning by back-propagation, whereby the data are repeatedly shown to the network until satisfactory learning is achieved. The error function is

$$E^{(k)} = \sum_{i=1}^{N_{dat}} \frac{\left(F_i^{(art)(k)} - F_i^{(net)(k)} \right)^2}{\sigma_{s,i}^{(exp)2}}, \quad (3.26)$$

where $F_i^{(net)(k)}$ is the prediction for the i -th data point from the net trained on the k -th replica of the data. Use of this error functions, which only includes statistical errors, ensures [12]

that statistical errors on adjacent data points are correctly combined, whereas the correlated systematics are reproduced when averaging over the Monte Carlo sample.

3.4 Results and validation

In Ref. [12], an independent set of neural networks was trained on the non-singlet combination $F_i^{(p)} - F_i^{(d)}$. This procedure is advisable because the structure functions are roughly of the same size, while their difference is typically by a factor 10 smaller. The length of training is fixed by studying the behaviour of the error function $E^{(0)}$, defined as in eq. (3.26) for the neural net fitted to the central experimental values, and asking that $E^{(0)}/N_{dat}$ stabilizes to a value close to one.

A number of checks is then performed in order to make sure that an unbiased representation of the probability density has been obtained. For instance, it has been verified that the covariance of two data points computed from the Monte Carlo sample of nets is on average very close to the corresponding covariance matrix element of the data. Since correlations of the data are entirely due to systematics, this indicates that the systematics is correctly reproduced.

It turns out that the average standard deviation for each data point computed from the Monte Carlo sample of nets is substantially smaller than the experimental error. This could be due to the fact that the network is combining the information from different data points by capturing an underlying law, or that it is introducing a smoothing bias. In Ref. [12] a statistical indicator which distinguishes the two cases was constructed: define

$$\tilde{E}^{(k)} = \sum_{i=1}^{N_{dat}} \frac{\left(F_i^{(exp)(k)} - F_i^{(net)(k)}\right)^2}{\sigma_{i,s}^{(exp)^2}}, \quad (3.27)$$

i.e. a modified error function where the prediction of the k -th net for the i -th point is compared to the central experimental value rather than to the k -th replica. The desired indicator is

$$\mathcal{R} \equiv \frac{\langle \tilde{E} \rangle_{rep}}{\langle E \rangle_{rep}}, \quad (3.28)$$

where $\langle \rangle_{rep}$ denotes the average over the ensemble of replicas, and E, \tilde{E} are respectively defined by eqs. (3.26) and (3.27). One can then show that, in the limit in which the error computed from the Monte Carlo sample is much smaller than the experimental one, $\mathcal{R} \approx 1/2$ if an underlying law is captured by the net, but $\mathcal{R} \gtrsim 1$ if the error reduction is due to a smoothing bias. The Monte Carlo sample of nets of Ref. [12] has $\mathcal{R} = 0.58$.

The final set of neural networks $F_i^{(net)(k)}$ provides a representation of the probability measure in the space of structure functions, which can be used to estimate any functional average, defined as in eq. (3.24), using

$$\langle \mathcal{F} [F_2(x, Q^2)] \rangle = \frac{1}{N_{rep}} \sum_{k=1}^{N_{rep}} \mathcal{F} [F_2^{(net)(k)}(x, Q^2)] . \quad (3.29)$$

In particular, the average, variance, and covariance of truncated moments computed using the Monte Carlo sample will give us a determination of values, errors and correlations of the measured truncated moments.

n	2	3	4	5	6	σ (%)
2	1.0	0.966	0.895	0.808	0.718	8.8
3	0.966	1.0	0.977	0.923	0.854	7.5
4	0.895	0.977	1.0	0.983	0.941	7.4
5	0.808	0.923	0.983	1.0	0.987	8.0
6	0.718	0.854	0.941	0.987	1.0	8.9

Table 1:

Errors and correlations for various truncated moments with $x_0 = 0.03$ and $Q^2 = 20 \text{ GeV}^2$.

Q^2	20	27.4	37.4	51.2	70	σ (%)
20	1.0	0.972	0.900	0.814	0.743	7.9
27.4	0.972	1.0	0.977	0.926	0.870	7.2
37.4	0.900	0.977	1.0	0.984	0.950	7.1
51.2	0.814	0.926	0.984	1.0	0.988	7.3
70	0.743	0.870	0.950	0.988	1.0	7.3

Table 2:

Errors and correlations for the fourth truncated moment with $x_0 = 0.03$ at various scales $20 \leq Q^2 \leq 70 \text{ GeV}^2$.

4 Determination of α_s

Using the neural parametrization of structure functions, we can compute directly experimental values of truncated moments at any scale in the region of the data. Because the neural parametrization retains all the experimental information, and specifically it allows a determination of errors and correlations, we can view such values as direct experimental determinations of the truncated moments. The value of α_s can then be extracted from scaling violations of truncated moments. Specifically, given the full set of truncated moments at a reference scale, the value of any truncated moment at any other scale is predicted in terms of α_s . Hence, we can obtain a determination of α_s by comparing this prediction with the data, for any choice of moment and scale. Even though such predictions are clearly correlated, it is to be expected that the use of a larger number of moments or scales will in general lead to a more precise determination of α_s ; the accuracy should, however, saturate for a large enough number of moments and scales. Errors and correlations for typical truncated moments are displayed in Tables 1 and 2. Correlations are quite large, so it is conceivable that an optimal fit may be obtained with a relatively small number of moments.

It is clear that to achieve a best fit for the strong coupling we must optimize the choice of the fitting procedure and parameters. We now turn to a detailed explanation of our choices for the truncation point of Mellin moments, for the range and number of scales Q^2 , for the number of moments to be used in the approximate evolution equation, the number of moments that should be treated as free parameters, and the effect of variations of these choices. We will then give our best fit with its associated statistical error. Finally, we will address the known sources

of theoretical error.

4.1 Choice of truncation point and fitting range

The choice of values of (x_0, Q^2) and of the moments to be used for the extraction of α_s is determined by the kinematic coverage of the data (see Fig. 1), as reflected by the errors on the moments. In particular, at low Q^2 there are no large x data, while at high Q^2 there are no small x data. In view of the fact that the use of truncated moments allows one to exclude the small x region, and that at low Q^2 power corrections can be sizable, it is convenient to consider only the large Q^2 region. Also, the large x extrapolation is severely constrained by the kinematic bound $F_2(1, Q^2) = 0$, whereas the small x behaviour is essentially unknown [20]. A reasonable cut which ensures a good coverage of the large x region is $Q^2 \geq 20 \text{ GeV}^2$. By choosing a high enough truncation point, $x_0 \gtrsim 0.3$, it would be possible to compute accurately truncated moments up to the highest available scale $Q^2 \approx 200 \text{ GeV}^2$. Such a choice, however, is not advisable, because the bulk of the data would then be excluded. In fact, as x_0 is raised, correlations between truncated moments rapidly increase. The value of x_0 should thus be chosen as small as possible, in order not to lose information. Requiring x_0 to be as low as $x_0 = 0.03$ imposes then a cut $Q^2 \leq 70 \text{ GeV}^2$. Smaller values of x_0 would require extrapolation.

We take thus as a baseline choice $x_0 = 0.03$, $20 \leq Q^2 \leq 70 \text{ GeV}^2$. With this choice, moments $1 < n < 8$ have errors below 10%, and correlation coefficients are below 0.9, as long as neighbouring moments are avoided, and one does not consider more than three (logarithmically) equally spaced scales in the available Q^2 range. Correlations between moments are not significantly reduced by further lowering x_0 , which would anyway require extrapolation. If, however, x_0 is raised to $x_0 = 0.1$, then correlations between neighbouring moments are greater than 0.98, and only correlations between moments differing by more than two orders are below 0.9. Because correlations between the same moment evaluated at different scales cannot be reduced without enlarging the Q^2 range, no more than three scales should be used if we wish to keep such correlations below 0.9. We will later consider variations of x_0 , the Q^2 range and the number of scales about this choice.

4.2 Evolution equation

As discussed in section 2, the scale dependence of any truncated moment $q_n(x_0, Q^2)$ can be determined to any required accuracy from the knowledge of a finite set of truncated moments at a reference scale Q_0^2 . The result has the form

$$q_n^{th}(x_0, Q_i^2) \equiv \sum_{p=n_{min}}^M M_{np}(x_0; Q_0^2, Q_i^2; \alpha_s) q_p(x_0, Q_0^2) , \quad (4.30)$$

where the evolution matrix M_{np} , explicitly given in Refs. [10, 11], is determined as a perturbative expansion in α_s .

Given a measurement of truncated moments $q_n^{exp}(x_0, Q^2)$ at more than one scale, the value of α_s can be determined by minimizing

$$\chi^2 = \sum_{n,i} \sum_{m,j} \left[q_n^{exp}(x_0, Q_i^2) - q_n^{th}(x_0, Q_i^2) \right] V_{ni;mj}^{-1} \left[q_m^{exp}(x_0, Q_j^2) - q_m^{th}(x_0, Q_j^2) \right] , \quad (4.31)$$

n	$x_0 = 0.1$	$x_0 = 0.03$	$x_0 = 0.01$
2	0.091 ± 0.047	0.085 ± 0.070	0.089 ± 0.080
3	0.100 ± 0.024	0.106 ± 0.030	0.106 ± 0.031
4	0.113 ± 0.019	0.115 ± 0.019	0.115 ± 0.019
5	0.122 ± 0.015	0.123 ± 0.015	0.123 ± 0.015
6	0.127 ± 0.014	0.127 ± 0.014	0.127 ± 0.014
7	0.129 ± 0.015	0.129 ± 0.014	0.129 ± 0.015
8	0.129 ± 0.016	0.129 ± 0.016	0.129 ± 0.016
9	0.129 ± 0.018	0.129 ± 0.018	0.129 ± 0.018

Table 3:

Fits of $\alpha_s(M_Z)$ from the evolution of a single moment.

where $V_{ni;mj}$ is the covariance matrix for moments $q_n^{exp}(x_0, Q_i^2)$, $q_m^{exp}(x_0, Q_j^2)$. Of course, the result for α_s should be independent of the choice of initial scale Q_0^2 .

If knowledge of moments $q_n(x_0, Q_0^2)$ with $n_{min} \leq n \leq M$ is needed in order to obtain the desired accuracy in the solution of the evolution equation, then in principle all these moments should be treated as free parameters in the minimization, along with the value of α_s , so the sum over n, m in eq. (4.31) should run from n_{min} to M . In practice, however, for any reasonable value of x_0 (say, $x_0 \lesssim 0.1$), the evolution of truncated moment $q_n(x_0, Q_0^2)$ is “almost diagonal”, in the sense that it receives only a small correction from moments $q_m(x_0, Q_0^2)$, with $m \neq n$. Because of this, and because of the large correlations between different moments, we may perform the minimization while only including a subset of moments in the sum over n, m in eq. (4.31), and treating only such moments as free parameters. This issue is discussed in detail in the next subsection.

Throughout this section, evolution will be performed using the improved method of Ref. [11], discussed in section 2.3. Specifically, we will take $n_{min} = 1$, with twelve moments included in the evolution equation ($M = 11$), while the reconstruction of $q(x_0, Q_0^2)$ according to eq. (2.21) will be performed with $N = 6$. This ensures an accuracy of order 0.1% on the evolution of the second ($n = 2$) truncated moment, rapidly improving as n increases. For α_s , we use the solution of the next-to-leading order renormalization group equation to express $\alpha_s(Q^2)$ in terms of $\alpha_s(M_Z)$, which is then directly taken as a free parameter. The number of active flavors varies by one unit at each quark threshold, and the coefficients of the β function are matched according to the Marciano [21] prescription. Dependence on quark thresholds will be studied as a source of theoretical uncertainty in section 4.6.

4.3 Choice of fitted moments

Having fixed the number of truncated moments to be included in the evolution equation, one still has to choose which ones should be treated as free parameters in the minimization procedure, and which ones should be fixed at the experimental central value. The simplest possibility is to fit only one moment at a time. The results for α_s obtained in this case are displayed in Table 3, with the default choice of scales, and three different choices of truncation point x_0 .

$x_0 = 0.03$	
Fitted moments	α_s
3+4	0.137 ± 0.011
2+4	0.140 ± 0.010
3+5	0.136 ± 0.011
4+6	0.131 ± 0.012
5+7	0.128 ± 0.012

Table 4:
Fits of $\alpha_s(M_Z)$ from the evolution of a pair of moments.

The table shows that the uncertainty in the determination of α_s , as a function of the order of the moment n , has a minimum around $n \approx 6$. The presence of a minimum can be understood as a consequence of the fact that the most accurate data have large $x \approx 0.5$, but there are no data with $x > 0.75$; furthermore, the anomalous dimension vanishes at low $n \sim 1$ (it vanishes exactly at $n = 1$ when $x_0 = 0$), and increases monotonically in modulus as n increases. Hence, low moments lead to a less precise determination both because they are dominated by small x data and because their scaling violations are weaker; for high enough n , on the other hand, there is loss of precision due to the extrapolation in the very large x region. In particular (see also below) moments with $n > 9$ probe a region of x where elastic contributions to the cross-section start being relevant, and become rapidly unreliable as n increases.

It is interesting to observe that all the determinations of Table 3 are compatible within errors. Also, it is interesting to observe that, for the values of n which give a reasonably precise determination of α_s , there is little or no dependence on the choice of x_0 of both the central value and the error. The error on any of these individual determinations is however much larger than the error obtained from existing fits to these data [22, 23]: a more accurate determination can only be obtained by combining the information from different truncated moments, *i.e.* fitting more than one truncated moment at a time.

When including more than one moment in the sum of eq. (4.31), the issue of correlations between moments becomes important. The impact of correlations is illustrated by the results obtained fitting a pair of moments, displayed in Table 4. Because of large correlations, in each case the value of α_s turns out to be larger than either of the values obtained from each of the two moments individually.

The presence of large correlations entails two distinct problems when performing a fit where several moments are simultaneously fitted. The first problem is that, as the elements of the covariance matrix $V_{ij} \rightarrow 1$, the matrix becomes singular, in that all eigenvalues but one vanish in the limit. Hence, when correlations are large, several eigenvalues become very small and the inversion of the covariance matrix is numerically problematic. The second problem is that, even if the covariance matrix is accurately inverted, when correlations are large, off-diagonal terms in the χ^2 eq. (4.31) may dominate over diagonal ones, thereby leading to generally unreliable and often pathological results. In particular, it may turn out that the best-fit values of all moments differ from the measured values by several standard deviations. An example of this pathological

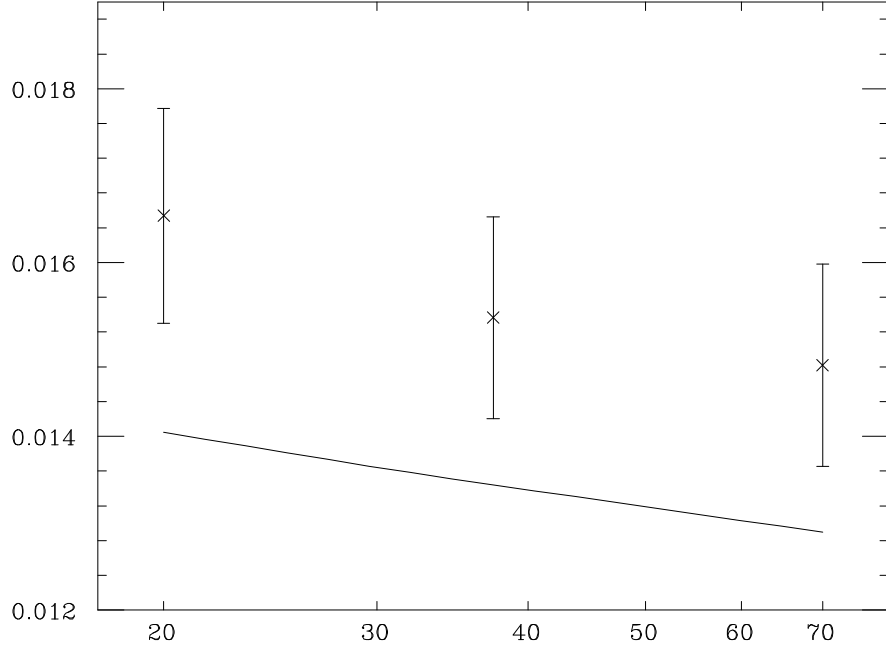


Figure 2:
Pathological best fit of the third moment in the presence of off-diagonal instabilities.

situation is displayed in Fig. 2, which shows the best-fit behaviour of the third moment ($n = 3$) in a fit of moments $2 + 3 + 4 + 5 + 6$, chosen as a representative case in which moments are over-correlated because too many neighbouring moments are fitted.¹ Even though this situation is in principle acceptable, in practice such results are unreliable because the minimum of the χ^2 is obtained by a fine-tuned balance of diagonal and off-diagonal contributions, which cannot be trusted whenever errors and correlations are known with limited accuracy [25]. We will refer to this situation as *off-diagonal instability* of the fits.

Because of these problems, there is a trade-off in accuracy when including more than one moment in the fit: the addition of more moments brings in new information, thus reducing statistical errors, but for a large enough number of moments it is impossible to accurately invert the covariance matrix, and fits are spoiled by instabilities. Whereas it is possible to keep the covariance matrix inversion under control by improving the numerical accuracy of calculations, the off-diagonal instability depends on the accuracy in the experimental determination of errors and correlations, and it is unavoidable. We have thus made sure that the covariance matrix is inverted to an accuracy which is by several orders of magnitude greater than the knowledge of its individual matrix elements. Then, we have tested for off-diagonal instabilities by flagging all results in which, at the best fit, one or more moments differ by more than one standard deviation from the experimental central value at any of the fitted scale, and discarding fits for

¹Note that even though this pathological situation is reminiscent of the effect which is found when linearizing correlated normalization errors [26], it is a distinct problem. To check this, we have replaced in the χ^2 eq. (4.31) all q_n with $\ln q_n$, and computed the covariance matrix accordingly. In such case normalization uncertainties decouple, yet we have verified that off-diagonal instabilities are still present.

$x_0 = 0.03$	
Fitted moments	α_s
2+3+4	0.126 ± 0.010
2+4+6	0.140 ± 0.008
3+5+7	0.138 ± 0.009
2+4+6+8	0.142 ± 0.009
3+5+7+9	0.124 ± 0.007
2+4+5+7	0.141 ± 0.009
3+4+5+6+7	0.1256 ± 0.0049
3+4+5+6+8	0.1247 ± 0.0050
2+4+5+6+8	0.1242 ± 0.0042
2+4+5+7+8	0.1254 ± 0.0044

Table 5:

Fits of $\alpha_s(M_Z)$ from the evolution of an increasing number of moments, with optimal x_0 .

which this happens for more than one experimental point.

Clearly, the maximum number of moments which may be included in the fit before an off-diagonal instability appears will be larger when correlations are lower. This means that first, it is not advantageous to further increase the number of scales beyond three (compare with Table 2); second, it is convenient not to fit simultaneously neighbouring moments (compare with Table 1); finally, it is convenient to choose a value of x_0 which is as low as possible since, as discussed above, correlations rapidly increase with x_0 . Indeed, we find that, with three scales and $x_0 = 0.03$, fits of up to five moments are possible, while with $x_0 = 0.1$ fits of at most four moments are possible without incurring in instabilities. With $x_0 = 0.01$ fits of up to seven moments are possible, but this choice of x_0 requires a considerable amount of extrapolation.

The results for representative fits with $x_0 = 0.03$ are shown in Table 5 as an increasing number of moments is fitted. It is clear that both the size of the error and the stability of the central value improve as the number of fitted moments increases. Stability of the central value of $\alpha_s(M_z)$ is found with the largest number of fitted moments allowed before the onset of off-diagonal instabilities.

4.4 Variation of the fit parameters

We now turn to the effect of variations of the truncation point x_0 and of the range and number of scales. Comparing the results of Table 5 with those obtained with a larger value of x_0 shows that with higher x_0 it is not possible to achieve satisfactory stability of the best-fit value of α_s before the onset of off-diagonal instabilities. Some representative results obtained with $x_0 = 0.1$ are displayed in Table 6; similar results are obtained for other values $x_0 > 0.03$. If instead x_0 is lowered to $x_0 = 0.01$ or below, the error on the best-fit α_s does not improve further, despite the fact that fits with a larger number of moments are possible, and remains in fact somewhat larger than the best fit of Table 5. This is consistent with the fact that lowering x_0 below 0.03 does not introduce any new experimental information.

$x_0 = 0.1$	
Fitted moments	α_s
2+3+4	0.128 ± 0.008
2+4+6	0.120 ± 0.010
3+5+7	0.121 ± 0.015
2+4+6+8	0.137 ± 0.008
3+5+7+9	0.140 ± 0.012
2+4+5+7	0.114 ± 0.009

Table 6:

Fit of $\alpha_s(M_Z)$ from the evolution of an increasing number of moments with large x_0 .

Q^2 range (GeV ²)	α_s
20-70	0.1242 ± 0.042
20-100	0.1239 ± 0.049
30-70	0.1239 ± 0.052
30-100	0.1249 ± 0.059

Table 7:

Dependence of the value of α_s on the Q^2 range for the $2 + 4 + 5 + 6 + 8$ fit with $x_0 = 0.03$

Coming now to scale choices, the first issue is the dependence of our results on the reference scale Q_0^2 . If we were fitting all moments, results would be entirely independent of this scale, except insofar as different choices of Q_0^2 correspond to different choices for the first guess of the values of the moments in the minimization routine. However, since only a subset of moments is fitted, there might be a residual dependence on Q_0^2 , due to the fact that the scale dependence of the central values of the moments which are not fitted might not agree completely with the predicted scale dependence. We have found that, in fact, the choice of initial scale may affect the onset of off-diagonal instabilities: for instance, the fit of moments $2 + 4 + 5 + 6 + 8$ turns unstable if $Q_0^2 > 40$ GeV². This is not surprising, in view of the fact that the central values of low moments are less accurate at this scale, because of the need to extrapolate at small x . Indeed, the instability does not appear if evolution is performed using the method of Ref. [9], instead of that of Ref. [11]: that method is less accurate, but it does not require knowledge of low moments since the evolution matrix is triangular (as discussed in section 2). Nevertheless, we find that, in all cases in which a stable fit is obtained, the results turn out to be essentially independent of the choice of the reference scale Q_0^2 .

Next, we consider the dependence on the choice of fitting scales. The range of scales cannot be widened much without requiring considerable extrapolation. The effect of small variations is displayed in Table 7. It is apparent that no significant dependence is found, and in fact the smallest error is obtained when $20 \leq Q^2 \leq 70$ GeV². If instead the number of scales is varied, we find that with only two scales the quality of the fit deteriorates considerably: for instance, the error on α_s from the fit of moments $2 + 4 + 5 + 6 + 8$ with $x_0 = 0.03$ goes up to $\sigma = 0.0077$ if only two scales are used. If four or more scales are used, fits with five moments become

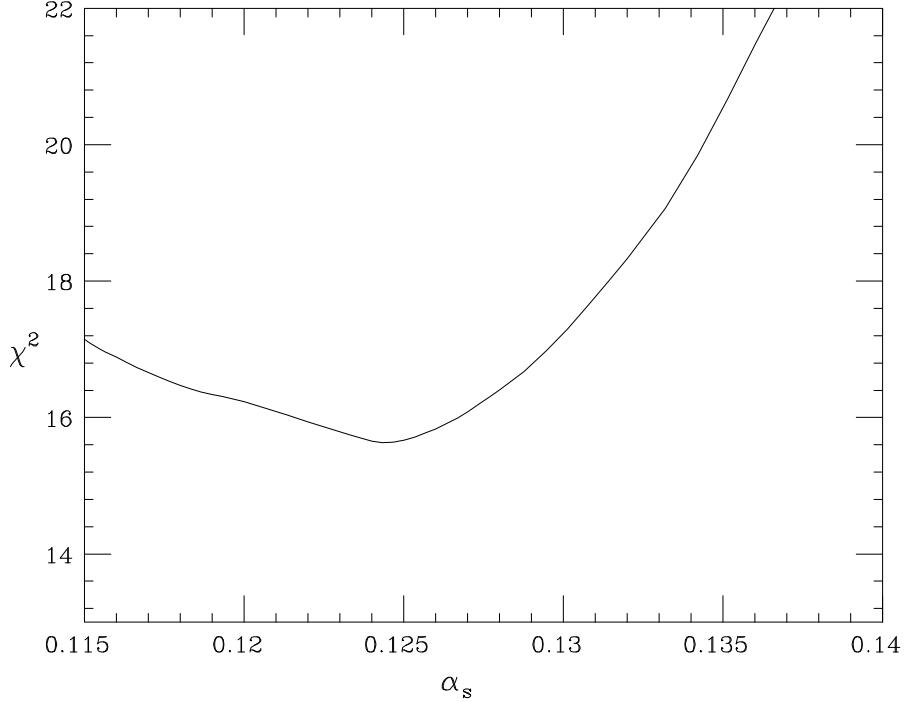


Figure 3:

χ^2 as a function of $\alpha_s(M_Z)$ for the fit of moments $2 + 4 + 5 + 6 + 8$ with $x_0 = 0.03$.

unstable because of excessive correlations, and it becomes impossible to find a stability region. Hence the choice of three scales in the range $20 \leq Q^2 \leq 70 \text{ GeV}^2$ appears to be optimal.

4.5 Best fit

Having tested how the quality of the fit varies with all the choices enumerated in the previous subsections, we select the fit architecture that maximizes the stability and minimizes the error. Our conclusion is that a reliable and stable determination of $\alpha_s(M_Z)$ is obtained with $x_0 = 0.03$, five moments (Table 5) and three scales $20 \leq Q^2 \leq 70 \text{ GeV}^2$. Specifically, the smallest error is obtained with the ‘symmetric’ combination of moments $2 + 4 + 5 + 6 + 8$, which we take as our baseline result. Note that the central value of α_s coincides with that which is obtained from single-moment fits (Table 3) when the error is stationary, *i.e.* for $5 \leq n \leq 6$. In order to obtain a more accurate determination of the statistical error, we have studied the dependence of the χ^2 on the value of α_s , displayed in Fig. 3. The χ^2 is asymmetric about the minimum, rising more slowly as α_s decreases. We arrive thus at the determination

$$\alpha_s(M_Z) = 0.124 \pm_{-0.007}^{+0.004} (\text{stat.}) . \quad (4.32)$$

4.6 Theoretical uncertainties

The main sources of theoretical uncertainty are higher-order perturbative and higher-twist corrections, as well as heavy quark threshold effects. First of all, our fits are based on leading-twist evolution of structure functions, so one should worry about possible power corrections. The largest corrections of this kind are target mass corrections, which are known analytically [27]. We have checked that these corrections are less than 1% on any of the moments included in our fits. Because higher-twist corrections to the operator product expansion are known [28] to be significantly smaller than target-mass corrections, we conclude that all power corrections are entirely negligible in our analysis, thanks to the relatively high cut $Q^2 \geq 20 \text{ GeV}^2$ which we have imposed. Also, one might worry that very high moments might be sensitive to elastic contributions to the cross section [29]. We have verified that such contributions are below 1% for all moments if $Q^2 \geq 30 \text{ GeV}^2$, and reach at most 3% for the 8-th moment at $Q^2 = 20 \text{ GeV}^2$, which is the highest fitted moment. We conclude that these contributions are also negligible. Nuclear corrections to the deuterium structure function affect the initial values of the fitted moments but not their scale dependence, and are thus immaterial, up to nuclear higher twist corrections, which are not expected to be significantly larger than standard higher twist terms (except possibly at very small x) [30].

We are then left with uncertainties related to higher-order perturbative corrections and to heavy quark thresholds. The position of thresholds $Q^2 = k_{th} M_q^2$ has been varied in the range $0.3 \leq k_{th} \leq 4$. Higher-order corrections have been estimated by varying the renormalization scale $\mu_{ren}^2 = k_{ren} Q^2$ in the standard way [31], with $0.3 \leq k_{ren} \leq 4$. Notice that, because the structure function is evolved directly in the DIS scheme [13], there is no factorization scale dependence. The χ^2 of the fit is almost independent of the choice of k_{th} , while it tends to increase considerably if $k_{ren} < 0.5$ or $k_{ren} > 2$; in particular, with $k_{ren} \leq 0.25$ we were unable to obtain a stable fit.

The dependence of the value of $\alpha_s(M_Z)$ on k_{th} and k_{ren} for the fit of moments $2+4+5+6+8$ with $x_0 = 0.03$ and three scales is displayed in Figure 4. The associated uncertainties are estimated to be

$$\sigma(\text{thresh.}) = {}^{+0.000}_{-0.002} ; \quad \sigma(\text{ren.}) = {}^{+0.003}_{-0.004} . \quad (4.33)$$

The dependence on the position of thresholds is, predictably, very weak, given that the b threshold is close to the edge of our Q^2 range, and falls outside it as soon as $k_{th} < 0.8$. The dependence on renormalization scale turns out to be also reasonably weak.

4.7 Result and comments

Our final determination of the strong coupling is

$$\alpha_s(M_Z) = 0.124 {}^{+0.004}_{-0.007} (\text{exp.}) {}^{+0.003}_{-0.004} (\text{th.}) = 0.124 {}^{+0.005}_{-0.008} (\text{total}) . \quad (4.34)$$

The error on the result is dominated by statistical uncertainties, consistent with our expectation that the method of analysis used here minimizes theoretical uncertainties.

The value of α_s has been previously extracted from QCD fits to the BCDMS data, with the result [22] $\alpha_s(M_Z) = 0.113 \pm 0.003(\text{exp.}) \pm 0.004(\text{th.})$, and to the NMC data, with the result [23] $\alpha_s(M_Z) = 0.117 {}^{+0.011}_{-0.016}$. There are two main differences between these previous determinations

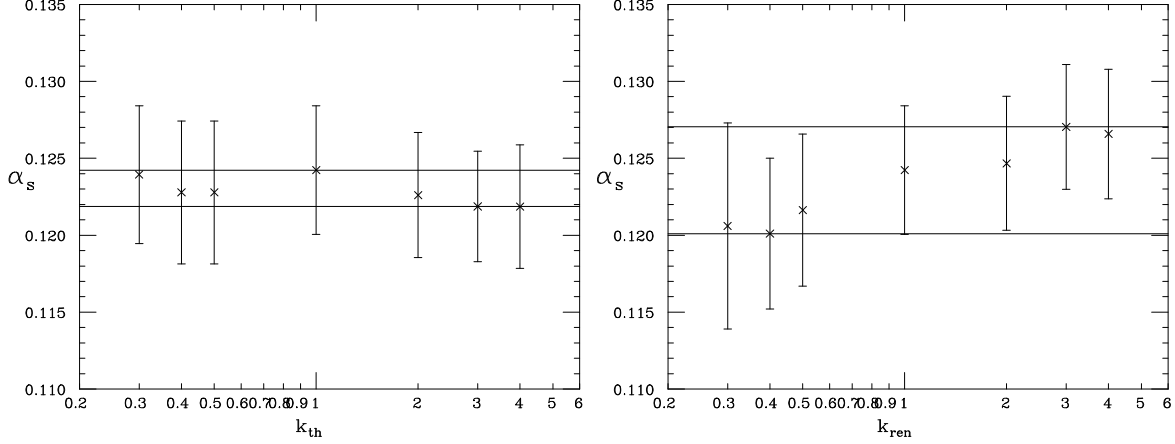


Figure 4:

Dependence of the best-fit value of $\alpha_s(M_Z)$ on the position of heavy quark thresholds (left) and renormalization scale (right). The band indicates the overall uncertainty.

and the present one, eq. (4.34). First, the determinations in Refs. [22,23] were based on global QCD fits, and thus required the construction of a parton parametrization, which, as discussed in the introduction, might be the source of systematic error and bias. Second, they did not include a full treatment of correlated systematics: statistical and systematic errors were added in quadrature. A reanalysis of the BCDMS data which did include a treatment of correlated systematics found instead [24] $\alpha_s(M_Z) = 0.118 \pm 0.002$ (exp.). Our value appears thus in good agreement with other determinations from the same data. While a direct comparison of the uncertainties is difficult, we find it interesting that, while the overall uncertainty of our value is very close to that of the BCDMS determination [22], our analysis gives excellent control on theoretical uncertainties: the dominant error is experimental and could be improved upon by future experiments.

It is interesting to observe that the central value we find, though in agreement within error with current global averages, is on the high side. As it appears from Table 3, the central value of α_s tends to be higher for higher moments. This is very suggestive of soft gluon resummation effects: as is well known [32], leading higher order corrections at large N are resummed by the replacement $Q^2 \rightarrow Q^2/N$ in the argument of α_s in the evolution equation for the N -th (full) moment. This means that the effective value of α_s is larger for the evolution of higher moments. Our results provide some indication of this effect, and suggest that a better determination of α_s could be obtained from these data if this resummation were included, by generalizing the soft gluon resummation formalism to the case of truncated moments. In particular, the inclusion of soft gluon effects to all orders is likely to reduce the theoretical uncertainty expressed by the dependence on the renormalization scale.

5 Concluding remarks

We have presented a determination of α_s from scaling violations aimed at minimizing the sources of theoretical bias which might be cause of concern in existing determinations of α_s from deep inelastic scattering experiments. This has been accomplished by avoiding the use of a parton parametrization: thanks to the use of truncated moments, we have directly fitted the scaling violations of a physical observable. Truncated moments in turn have been determined by means of a bias-free parametrization of the structure function, inferred from the data, which retains all the information on experimental errors and correlations.

It is interesting to compare our final result for α_s to other determinations from deep inelastic scattering, and in particular those obtained using the same data set [22–24]. Whereas in our determination theoretical errors are small and fully under control, the price to pay for this is that the experimental error is larger than in other determinations. It is unclear to which extent this is a trade-off, or a consequence of the need to impose restrictive cuts in the Q^2 range in order to deal with truncated moments. However, it does suggest that a substantially more precise determination could be obtained using data with either smaller statistical error (especially for deuteron data), or spanning a wider Q^2 range, or both, such as could be obtained for instance at the planned EIC facility [33].

As far as the central value of α_s is concerned, it is suggestive that our determination is on the high side, since this is what one would expect in the presence of sizable soft gluon resummation effects. These in turn are expected to be more important in our determination, since the kinematic cuts which we imposed give more weight to the large- x region, where such effects are larger. Therefore, we expect that a resummed version of our analysis might lead to a more accurate result for α_s , and provide explicit evidence for soft gluon resummation.

Finally, our analysis provides an explicit demonstration of the power of methods of analysis based on the direct determination of the probability density of physical observables from the data, and their use coupled with the bias-free computational method which is afforded by the use of truncated moments.

Acknowledgements

It is a pleasure to thank L. Garrido, who co-authored Ref. [12] and participated in many discussions along the course of this project. We also thank G. Altarelli, G. d’Agostini and G. Ridolfi for discussions. This work was supported in part by EU TMR contract FMRX-CT98-0194 (DG 12-MIHT) and by the Spanish and Catalan grants AEN99-0766, AEN99-0483, 1999SGR-00097.

References

- [1] See *e.g.* S. Catani *et al.*, in *CERN 1999, Proceedings* “Standard Model Physics (and more) at the LHC”, *CERN report CERN-2000-004*, [hep-ph/0005025](#);
S. Alekhin *et al.*, [hep-ph/0204316](#), to be published in *Les Houches 2001, Proceedings* “Physics at TeV Colliders”.
- [2] S. Bethke, *J. Phys.* **G26** (2000) R27, [hep-ex/0004021](#).
- [3] G. Altarelli, [hep-ph/0204179](#).
- [4] G. Altarelli and G. Parisi, *Nucl. Phys.* **B126** (1977) 298.
- [5] See *e.g.* R.K. Ellis, W.J. Stirling and B.R. Webber, “QCD and Collider Physics” (Cambridge, 1996).
- [6] See *e.g.* S. Forte, *Nucl. Phys.* **A666** (2000) 113.
- [7] G. Altarelli *et al.*, *Nucl. Phys.* **B496**, 337 (1997), [hep-ph/9701289](#); *Acta Phys. Pol.* **B29** (1998) 1145, [hep-ph/9803237](#).
- [8] W.T. Giele, S.A. Keller and D.A. Kosower, [hep-ph/0104052](#); also in *La Thuile 1999, Proceedings* “Rencontres de Physique de la Vallée d’Aoste”, p. 255 (INFN, Frascati, 1999);
W. T. Giele and S. Keller, *Phys. Rev.* **D58** (1998) 094023, [hep-ph/9803393](#).
- [9] S. Forte and L. Magnea, *Phys. Lett.* **B448** (1999) 295, [hep-ph/9812479](#); also in *Tampere 1999, Proceedings* “International Europhysics Conference on High-Energy Physics” (EPS-HEP 99), Tampere 1999, p. 454, [hep-ph/9910421](#).
- [10] S. Forte, L. Magnea, A. Piccione and G. Ridolfi, *Nucl. Phys.* **B 594** (2001) 46, [hep-ph/0006273](#).
- [11] A. Piccione, *Phys. Lett.* **B518** (2001) 207, [hep-ph/0107108](#).
- [12] S. Forte, L. Garrido, J.I. Latorre and A. Piccione, [hep-ph/0204232](#).
- [13] G. Altarelli, R. K. Ellis and G. Martinelli, *Nucl. Phys.* **B143** (1978) 521 [Erratum-*ibid.* **B146** (1978) 544]; *Nucl. Phys.* **B157** (1979) 461.
- [14] S.I. Alekhin, *Eur. Phys. J.* **C10** (1999) 395, [hep-ph/9611213](#);
D. Stump *et al.*, *Phys. Rev.* **D65** (2002) 014012, [hep-ph/0101051](#);
J. Pumplin *et al.*, *Phys. Rev.* **D65** (2002) 014013, [hep-ph/0101032](#).
- [15] F.J. Yndurain, *Phys. Lett.* **B74** (1978) 68;
G. Parisi, N. Surlas, *Nucl. Phys.* **B151** (1979) 421;
W. Furmanski, R. Petronzio, *Nucl. Phys.* **B195** (1982) 237.
- [16] M. Arneodo *et al.* (New Muon Coll.), *Nucl. Phys.* **B483** (1997) 3, [hep-ph/9610231](#).
- [17] A.C. Benvenuti *et al.* (BCDMS Coll.), *Phys. Lett.* **B223** (1989) 485; *Phys. Lett.* **B237** (1990) 592.

- [18] M.R. Adams *et al.* (E665 Coll.) *Phys. Rev.* **D54** (1996) 3006.
- [19] C. Peterson and T. R  gnvaldsson, *Lectures at the 1991 CERN School of Computing, preprint LU–TP–91–23*;
 B. M  ller, J. Reinhardt and M. T. Strickland, *Neural Networks: an introduction* (Berlin, 1995);
 G. Stimpfl–Abele and L. Garrido, *Comput. Phys. Commun.* **64** (1991) 46.
- [20] See *e.g.* S. Forte and R. D. Ball, *Acta Phys. Polon.* **B26** (1995) 2097, [hep-ph/9512208](#).
- [21] W.J. Marciano, *Phys. Rev.* **D29** (1984) 580.
- [22] M. Virchaux and A. Milsztajn, *Phys. Lett.* **B274** (1992) 221.
- [23] M. Arneodo *et al.*, *Phys. Lett.* **B309** (1993) 222.
- [24] S.I. Alekhin, *Phys. Rev.* **D59** (1999) 114016, [hep-ph/9809544](#).
- [25] G. Cowan, *Statistical data analysis*, (Oxford, 1998).
- [26] G. D’Agostini, *Nucl. Instrum. Meth.* **A346** (1994) 306.
- [27] See *e.g.* J.L. Miramontes and J. S  nchez–Guillen, *Z. Phys.* **C41** (1988) 247, and refs. therein.
- [28] U.K. Yang and A. Bodek, *Phys. Rev. Lett.* **82** (1999) 2467, [hep-ph/9809480](#).
- [29] A. Bodek, in *Blois 1994 Proceedings* “The heart of the matter”, p. 255.
- [30] See K. J. Eskola *et al.*, [hep-ph/0110348](#) and ref. therein.
- [31] See *e.g.* G. Ridolfi and S. Forte, *J. Phys.* **G25** (1999) 1555.
- [32] See *e.g.* S. Catani, M.L. Mangano, P. Nason and L. Trentadue, *Nucl. Phys.* **B478** (1996) 273, [hep-ph/9604351](#), and refs. therein.
- [33] A. L. Deshpande, *Nucl. Phys. Proc. Suppl.* **105** (2002) 178.